A molecular rack and pinion actuates a cell-surface adhesin and enables bacterial gliding motility

Authors: Abhishek Shrivastava and Howard C. Berg

Affiliation: Department of Molecular and Cellular Biology, Harvard University, Cambridge, MA 02138

Email: hberg@mcb.harvard.edu
& ashrivastava@fas.harvard.edu

Abstract. Motile but non-swimming bacteria achieve self-propulsion over surfaces using mechanisms that are barely understood. *Flavobacterium johnsoniae*, which exhibits some of the fastest motion of all known non-flagellated, non-piliated bacteria, has a mobile cell-surface adhesin, SprB, and a powerful rotary motor. The attachment of SprB to an external surface is required for bacterial gliding. How rotation might be coupled to the motion of SprB over the cell-surface is a puzzle. GldL, which is a component of the bacterial Type IX secretion system (T9SS) and is required for the secretion of SprB, localized at the axis of rotation of a tethered cell, suggesting that it is a part of the rotary motor. SprB moves along a spiral track that loops back as it reaches the cell pole. Is GldL close enough to such a track for a motor to engage a tread that moves along the track? We measured the proximity of GldL-YFP spots to tracks carrying Cy3-labeled SprB. The GldL spots and the labeled tracks were about 90 nm apart, a distance commensurate with the known rotation speeds and gliding rates. We propose a model in which a pinion, connected to a rotary motor, drives a rack (a tread) that moves along a spiral track fixed to the rigid framework of the cell wall. SprB, carried by the tread, adsorbs to the substratum and causes the cell to glide.

Significance. In mechanical devices, rotary motion can be converted to linear motion when a circular gear, called a pinion, engages a linear gear, called a rack. Is such machinery present in nature? The data presented here show that in certain bacteria that exhibit gliding motility, the axes of rotary motors are about 90 nm away from cell-surface tracks on which adhesins move. Gliding occurs when such adhesins adsorb to the substratum, e.g., glass. If 90 nm is the radius of a pinion rotating 3Hz (the

maximum speed of rotation when a cell is tethered) then that pinion can drive a rack (a tread carrying adhesins) at 1.5 μm/s, which is the speed that cells glide. This suggests that nature has not only invented the wheel, it also has invented the likes of a microscopic snowmobile.

Introduction. Rod-shaped gliding bacteria move in a manner similar to a self-propelled screw, i.e., they roll along their long axis as they move forward on an external surface (1, 2). Bacteria related to *Flavobacterium johnsoniae*, which is the fastest of all known gliders, are present in diverse environments such as the human oral microbiome, fish scales, water bodies, and plant roots, where they glide over their preferred surfaces. How the molecular players form the machinery that actuates this motion is not clearly understood. *Flavobacterium johnsoniae* is now the organism of choice for studies of this process, because rates of movement are high and much of the genetics is known (3, 4). A mobile cell-surface adhesin, SprB, has been identified that plays a central role in gliding (5, 6). Tracking of SprB in 3D space has revealed the presence of a spiral cell-surface track on which SprB moves (1). Cells subjected to viscous shear stop gliding, but they can be tethered to an external surface using anti-SprB antibody. Tethered cells pinwheel around a fixed axis, suggesting that a rotary motor that generates high torque is a part of the gliding machinery (7).

Bacterial motility machines have external components, so are coupled with protein secretion systems. The flagellar motor is associated with the Type 3 secretion system (8, 9), and the Type IV pili motor is associated with the type II secretion system (10-12). In *Flavobacterium*, the Type IX secretion system (T9SS) is required for the secretion of SprB, and cells lacking the T9SS are non-motile (3). The T9SS forms at least one ring-

shaped structure (13). GldL is a cytoplasmic membrane protein and is one of the core T9SS proteins (14). Our results suggest that the T9SS is associated with the rotary component of the gliding motor which drives a tread carrying the adhesin SprB along a track fastened to the rigid framework of the cell wall.

Results and Discussion.

The axis of rotation is localized near GldL. GldK, GldL, GldM, GldN, SprA, SprE, SprF and SprT are the core T9SS proteins required for the transport of SprB to the external surface. Δ*gldL* mutants lack SprB and are not able to stick to a glass surface (14). We found that Δ*gldL* mutants complemented by GldL-YFP were able to bind to glass and exhibited wild-type levels of cell rotation but did not move long distances on glass (Movie S1). This suggests that while the rotary motor is fully functional, the tread that carries SprB or the track on which it moves might not assemble properly in this strain. Un-sheared wild-type *F. johnsoniae* cells can sometimes self-tether onto a glass surface and exhibit rotation. However, such a tether is not very firm, as a result of which most un-sheared cells do not rotate for long time intervals. In contrast, sheared cells tether firmly and rotate for a long time (7). Presumably, shearing breaks down the tread on the cell surface, as a result of which SprB does not move along the length of the cell but stays near the rotary motor.

Fluorescent GldL-YFP appeared as spots or foci that were fixed in the frame of reference of a cell (Fig. 1A & Movie S2). About 3 GldL foci were found per cylindrical face of a cell, as measured from 42 cells (Fig. 1B). The TIRF microscope used for these measurements strongly illuminates only the cylindrical face of the cell adjacent to

the glass, but a similar distribution of GldL is expected on the opposite cylindrical face. So, the total number of GldL foci per cell is about 6. The GldL spots appeared to be localized at random, with the average distance between two neighboring spots about 1.5 μm (Fig. S1). The position of the axis of rotation was determined by adding successive phase-contrast images in a video of a rotating cell and fitting the average with a 3D gaussian (Fig. 1C). The axis of rotation of a tethered cell always was found near a GldL spot (Fig. 1D) as expected if GldL is a part of the rotary motor.

Cell rotation and SprB utilize the same power source. A preparation of tethered cells was exposed to 10 μM carbonyl cyanide-m-chlorophenylhydrazone (CCCP), which is known to abolish the protonmotive force that acts across the inner cell membrane (15). The cells stopped rotating after the addition of CCCP and started rotating again after its removal (Fig. S2, S3 and Movie S3). The loss of rotation was rapid and the recovery was gradual, taking about 4 times longer, as expected if time was required to wash CCCP out of the cells. These results are consistent with previous observations where motion of SprB was stopped after the addition of CCCP and was restored after washing it away (6). This suggests that both cell rotation and SprB are driven by the same fuel.

A22, a drug that alters the motion of MreB and stops the gliding of *Myxococcus xanthus* (16), did not affect the gliding of *F. johnsoniae*. As in *F. johnsoniae*, binding of a cell-surface adhesin to an external surface results in gliding of *M. xanthus*. However, there are obvious differences between the gliding of the two types of bacteria. *M. xanthus* uses different motility proteins and glides about 60 times more slowly than *F.*

johnsoaniae. Since MreB helps in building the cell wall to which the *F. johnsoniae* gliding machinery is attached, MreB might play a role in the assembly of that machinery.

The track on which SprB moves is close to the gliding motor. While the motor labeled by GldL-YFP is fixed on the cell surface, the SprB adhesin moves along the length of the cell. How rotation might be coupled to linear motion is a puzzle. A Cy3 tag was attached to SprB and the positions of both SprB and GldL were determined in the same cells (Fig 2A and Movie S4). The shortest distance between the trajectory of SprB labeled with Cy3 and motors labeled with GldL-YFP was measured for 42 motors in 10 cells. Most motors were at a distance (*d*) of about 90 nm from the SprB trajectory (Fig. 2B).

As a control, a simulation in which 42 motors were randomly localized in one cell was performed, together with the SprB trajectory from one cell. The shortest distances between the motors and the track were measured. The distribution for these distances was broad and did not show a discernible peak near 90 nm (Fig. S5).

Tracks carrying SprB did not loop around GldL spots. This argues against a model in which chains carrying SprB are driven by sprockets (4). A viable alternative, explained below, involves racks and pinions.

A model for gliding is suggested in which a pinion attached to the rotary motor's drive shaft engages a rack (a tread) that slides along a track fixed to the rigid framework of the cell wall. A cartoon illustrating this idea is shown in Fig. 3A. A pinion (a circular gear) and a rack (a straight element with teeth matching those on the gear) is a common device for converting rotary motion into linear motion. If the motor rotates at frequency *f* and the radius of the pinion is *r*, then the rack will move at velocity

$v = 2\pi rf$, which is the gliding speed, about 1.5 μm/s. Given the maximum f that the rotary motor exhibits of about 3 Hz (7), we find $r = v/2\pi f = 80$ nm, which is on the mark.

The rotary motor, although it runs at constant speed, could be similar in architecture to the flagellar rotary motor, with a rotor embedded in the inner cell membrane surrounded by stator elements anchored to the peptidoglycan layer and a drive shaft that passes through the peptidoglycan with the aid of a bushing. The pinion would be mounted on the drive shaft but could rotate under or within the outer cell membrane, driving the tread along a track anchored to the peptidoglycan. Only SprB need extend beyond the outer cell membrane. An animation of the behavior of our model is shown in Fig. 3B and Movie S5.

Multiple SprB's ensure smooth gliding. If several SprB are mounted on a given tread, a cell can glide continuously. Typically, there are 40 SprB on a given track, or 20 on one face of a cell. A SprB arriving at the back of a cell can peel off the substrate to be replaced by new SprB adsorbed to the substrate at the front of the cell. As a result, the cell can glide smoothly over many body lengths. However, if a single SprB is mounted on a given tread, that SprB will remain fixed and the free end of the cell will lift off the surface and flip over, allowing the cell to continue to glide in the same direction but without any net progress. Gliding cells often display flips, i.e., the lagging pole of a cell gliding in the x-y image plane gets stuck to glass, the leading pole rises up along the z axis and moves rapidly forming an arc such that it moves behind the lagging pole (Fig. S7 and Movie S5). The flips are illustrated in Fig. 1 and Movie S1 of ref. 4 and in Fig. 4 of ref. 17. At the time of the early work, no gliding motility proteins were known;

all that could be surmised was that sites able to adhere to the substrate moved the length of a cell along tracks fixed to the rigid framework of the cell wall.

Future experiments will be aimed towards identification of the proteins that comprise the gliding machinery. Several *F. johnsoniae* mutants are deficient in proteins that either form the T9SS or are involved in the stability of the T9SS proteins. In these mutants, SprB is not secreted to the cell-surface and the cells do not glide. Of more interest are mutants that do secrete SprB to the cell surface but, nonetheless, are not able to glide. An example are cells that lack the C-terminal region of GldJ (18), a protein that is not a part of the T9SS. GldJ localizes helically, is an outer membrane lipoprotein (19), and is presumably a part of the tread/track complex. Identification of other components of the rack and pinion assembly will enhance our understanding of gliding.

Methods.

Strains and plasmids. A GldL-YFP fusion was generated by amplifying eYFP from pHL55[20] using primers P65 and P67 (for primers, see Supplementary Information) and cloning it into the vector pCP23. *gldL* was amplified using primers P63 and P64 and was cloned into pCP23 with YFP to generate the plasmid pAS6 such that the C-terminal region of GldL was fused with the N-terminus of YFP. Strains were grown at 25˚C with shaking, as described previously (1).

TIRF imaging of GldL in tethered cells. To image rotating bacteria with GldL-YFP, a microscope (Nikon Eclipse Ti-U; Nikon, Melville, NJ) with an Apo TIRF 60x 1.49 numerical aperture (NA) objective was used in TIRF mode. A 515 nm, 25 mW laser

was used as an excitation source. Fluorescent images were recorded with an Andor Ixon Camera. Phase-contrast images were recorded at the same time in the near infrared using a ThorLabs DCC1545M-GL camera. Images were analyzed using the ImageJ plugin Trackmate and custom MATLAB codes.

TIRF imaging of SprB and GldL. To track the motion of SprB while marking the position of GldL in the same cell, a GldL-YFP-containing plasmid was added to wild-type cells to form a hybrid motor. Such cells had both wild-type GldL and GldL-YFP. Motion of SprB and gliding at wild-type levels were observed with this strain. SprB was labeled with Cy3 as follows: 2 μL of 1:10 diluted purified anti-SpB antibody and 2μL of Cy3 conjugated Goat Anti Rabbit IgG Polyclonal Antibody (VWR R611-104-122) were added to 40 μL of 0.4 O.D. bacterial culture and incubated for 10 min at 25˚C. After incubation, the preparation was centrifuged at 12,600 x g for 5 min. The supernatant fraction was discarded and the pellet was re-suspended in 40 μL of motility medium (MM). A tunnel slide was prepared, 40 μL of 10 mg/mL BSA was added to the tunnel and allowed to stand for 1 min, after which the Cy3-labeled cells were flowed into one end of the tunnel, and a Kimwipe was used to wick the excess fluid from the other end. This preparation was allowed to stand for 10 min, and then was washed twice in the tunnel slide with 40 μL of MM.

To image YFP and Cy3 signals simultaneously, the TIRF system described above was used with a Photometrics DV2 attachment with yellow and red filters (Chroma ET 535/30 and ET 630/75, respectively) to image YFP on one side of the screen and Cy3 on the other. Images were analyzed using ImageJ plugin Trackmate and a custom MATLAB code.

Addition of CCCP and A22. Wild-type *F. johnsoniae* cells were sheared and tethered to a glass coverslip and attached to a flow cell, and rotation speed was measured as described previously (7). A CCCP stock was prepared (10 μM in MM and added at the rate of 50 μL/min using a syringe pump (Harvard Apparatus 22). To remove the drug, MM was pumped into the flow cell.

A22 (50 μg/mL) was added to cells gliding on glass in a tunnel chamber as described previously. Cells were imaged using a phase-contrast microscope with a Nikon Plan 40x BM NA 0.65 objective (Nikon Melville, NY) and a Tholabs DCC1545M-GL (Thorlabs, Newton, NJ) camera. Images were analyzed using a custom MATLAB code.

Figure Legends.

Figure1. The axis of rotation is found near a GldL spot. (A) About 4 GldL foci appeared per cylindrical face of a cell. Five foci are shown here for one tethered cell, with the one numbered 5 close to the axis of rotation. The others execute circular arcs as the cell rotates. **(B)** The distribution of numbers of GldL foci per cell for 42 cells. The foci were spaced about 1.4 μm apart. (**C**) The axis of rotation of a tethered cell was determined using a 3D gaussian fit. (**D**) Distances of the GldL foci of the tethered cell shown in Fig.1A from the axis of rotation plotted as a function of time.

Figure 2. GldL localizes near the track on which SprB moves. (A) Co-localization of GldL (green circles) with the trajectory of SprB (blue dots and red line). GldL remains fixed relative to the cell. SprB moves along the trajectory shown in red. Blue dots mark the position of SprB observed at different time points. Red lines are second-order polynomial fits to the blue dots. GldL was labeled with YFP and SprB with Cy3. **(B)** Frequency distribution of the distance of 42 motors from SprB trajectories for 10 cells, showing a peak at a distance of about 100 nm.

Figure 3. A model of the gliding machinery. (A) A cross-sectional view of a cell with a rotary gliding motor (blue), a mobile tread (green), a stationary track (red), and an adhesin (magenta). The rotary motor and the track are anchored to the peptidoglycan (PG), and the track is wound spirally around the cell. The rotary motor drives a pinion that engages a mobile tread (rack) that slides along the track. The adhesin, SprB, is attached to the tread and moves with it. The dimension *d* is the distance between the axis of rotation of the motor and the center of the track, and *r* is the radius of the pinion. **(B)** A side view of a cell with a rotary motor powering the motion of a tread carrying SprB. See Movie S5 for an animation of this model.

Author Contributions: AS and HCB designed the experiments and wrote the paper. AS performed the experiments.

Acknowledgements: This work is supported by National Institutes of Health Grant AI016478 to HCB and a K99/R00 Grant DE026826 to AS.

References:

1 Shrivastava A, Roland T, Berg HC (2016) The screw-like movement of a gliding bacterium is powered by spiral motion of cell-surface adhesins. *Biophys J* **111**: 1008-1013.

2 Faure LM *et al.* (2016) The mechanism of force transmission at bacterial focal adhesion complexes. *Nature* **539**:530-535.

3 McBride MJ, Nakane D (2015) Flavobacterium gliding motility and the type IX secretion system. *Curr. Opin. Microbiol.* **28**:72-77.

4 Shrivastava A, Berg HC (2015) Towards a model for *Flavobacterium* gliding. *Curr. Opin. Microbiol.* **28**:93-97.

5 Nelson SS, Bollampalli S, McBride MJ (2008) SprB is a cell surface component of the *Flavobacterium johnsoniae* gliding motility machinery. *J. Bacteriol.* **190**: 2851-2857.

6 Nakane D, Sato K, Wada H, McBride MJ, Nakayama K (2013) Helical flow of surface protein required for bacterial gliding motility. *Proc Natl Acad Sci USA* **110**:11145-11150.

7 Shrivastava A, Lele PP, Berg HC (2015) A rotary motor drives flavobacterium gliding. *Curr Biol* **25**: 338-34.

8 Erhardt M, Namba K, Hughes KT (2010) Bacterial nanomachines: the flagellum and type III injectisome. *Cold Spring Harb Perspect Biol* **2**:a000299.

9 Blocker A, Komoriya K, Aizawa S (2003) Type III secretion systems and bacterial flagella: insights into their function from structural similarities. *Proc Natl Acad Sci. USA* **100**:3027-3030.

10 Chang YW et al. (2016) Architecture of the type IVa pilus machine. *Science* **351**: aad2001.

11 Skerker JM, Berg HC (2001) Direct observation of extension and retraction of type IV pili. *Proc Natl Acad Sci USA* **98**:6901-6904.

12 Cisneros DA, Pehau-Arnaudet G, Francetic O (2012) Heterologous assembly of type IV pili by a type II secretion system reveals the role of minor pilins in assembly initiation. *Mol Microbiol* **86**:805-818.

13 Gorasia DG et al. (2016) Structural Insights into the PorK and PorN Components of the *Porphyromonas gingivalis* Type IX Secretion System. *PLoS pathog* **12**: e1005820.

14 Shrivastava A, Johnston JJ, van Baaren JM, McBride MJ (2013) *Flavobacterium johnsoniae* GldK, GldL, GldM, and SprA are required for secretion of the cell surface gliding motility adhesins SprB and RemA. *J Bacteriol* **195**:3201-3212.

15 Harold FM, Baarda JR (1968) Inhibition of membrane transport in *Streptococcus faecalis* by uncouplers of oxidatve phosphorylation and its relationship to proton conduction. *J Bacteriol* **96**:2025-2034.

16 Mauriello EM et al. (2010) Bacterial motility complexes require the actin-like protein, MreB and the Ras homologue, MglA. *EMBO J* **29**:315-326.

17 Lapidus IR, Berg HC (1982) Gliding motility of *Cytophaga* sp. strain U67 *J Bacteriol* **151**:384-398.

18 Johnston JJ, Shrivastava A, McBride MJ (2017) Untangling *Flavobacterium johnsoniae* gliding motility and protein secretion. *J Bacteriol* epub ahead of print.

19 Braun T F, McBride MJ (2005) *Flavobacterium johnsoniae* GldJ is a lipoprotein that is required for gliding motility. *J Bacteriol* **187**:2628-2637.

20 Boehm A. et al. (2010) Second messenger-mediated adjustment of bacterial swimming velocity. *Cell* **141**:107-116.

Figure 1.

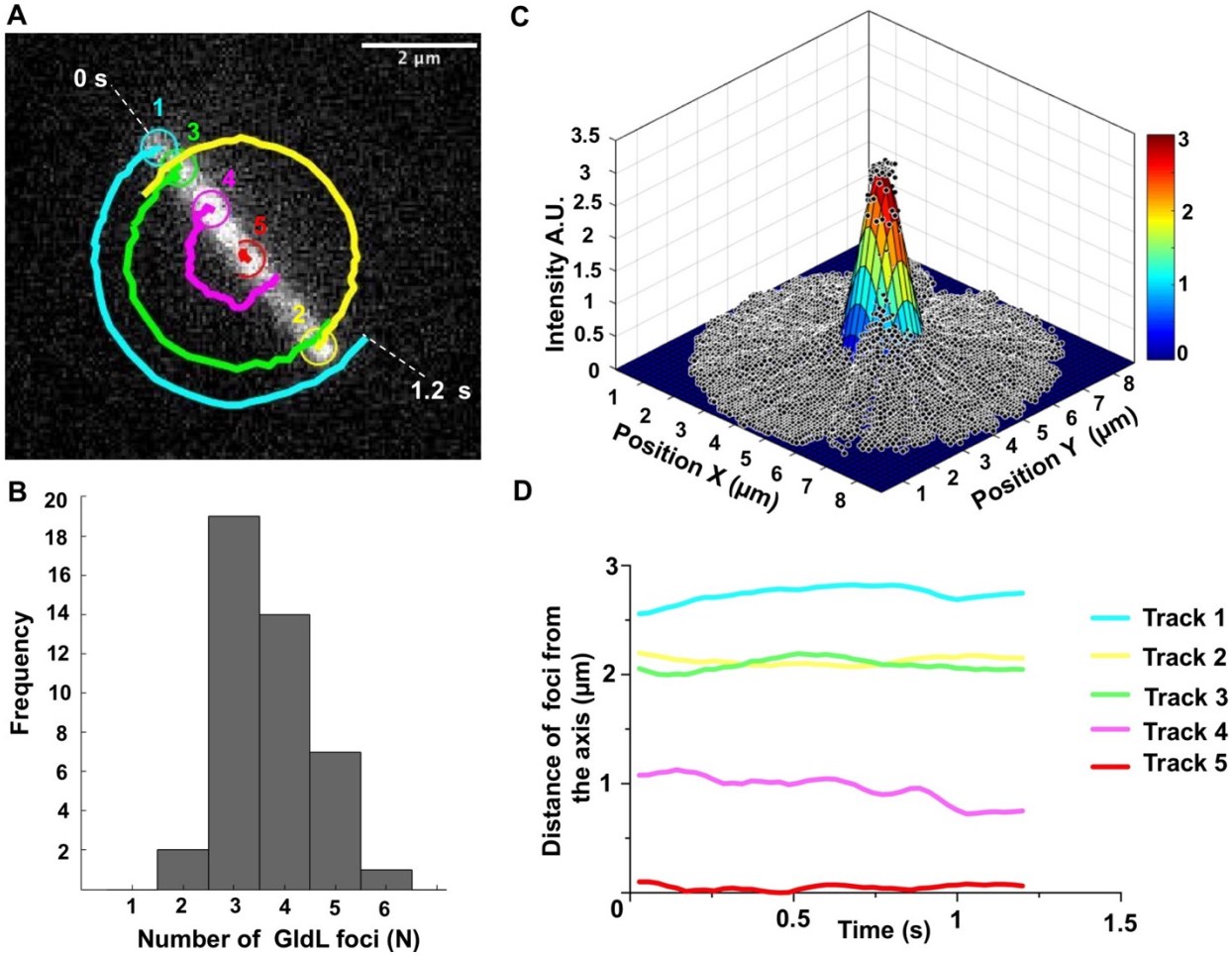
A
2 µm
0 s
1.2 s
1
2
3
4
5
B
Frequency
Number of GldL foci (N)
C
Intensity A.U.
Position X (µm)
Position Y (µm)
D
Distance of foci from the axis (µm)
Time (s)
Track 1
Track 2
Track 3
Track 4
Track 5

Figure 2.

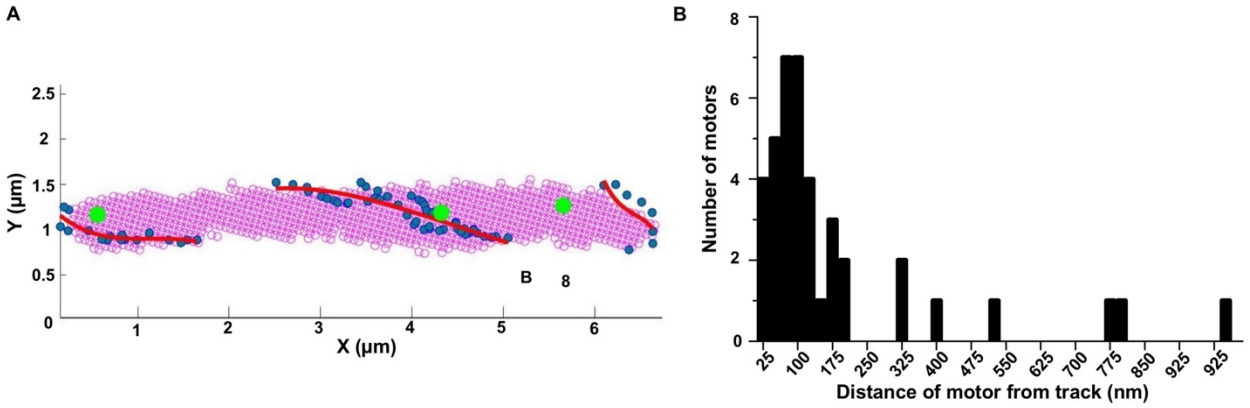

Figure 3.

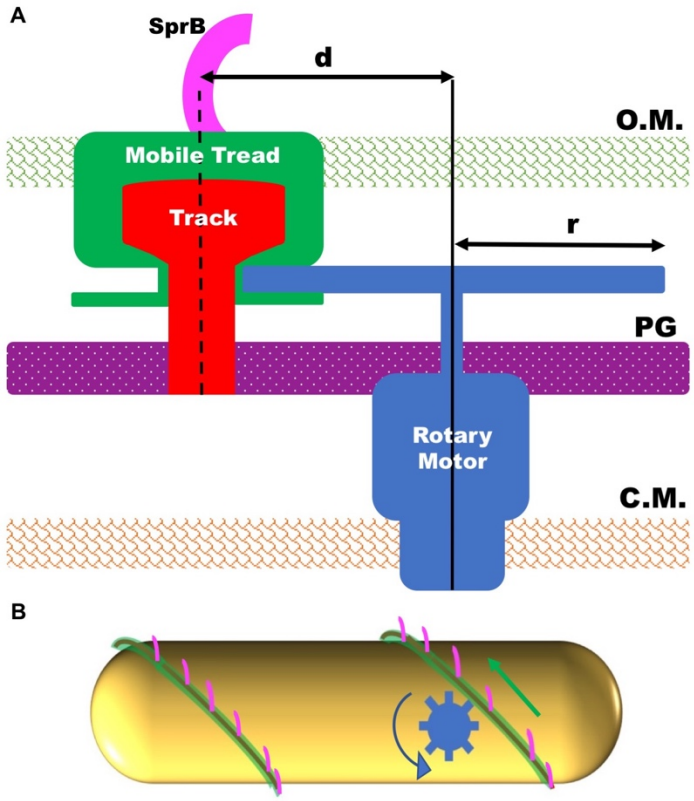

Supplementary Information.

Supplementary figure legends.

Figure S1. A frequency distribution of nearest-neighbor distances between 42 GldL foci found on 10 cells.

Figure S2. Rotation speed of a cell plotted as a function of time. Addition of CCCP stopped the rotation. Removal of CCCP restored the rotation.

Figure S3. The rate for the drop in rotation speed after addition of CCCP (red linear regression fit) is 4 times faster than the rate of increase following removal of CCCP (green fit).

Figure S4 Speed of a smooth gliding cell measured by tracking the center of mass does not change after the addition of A22. The sharp peaks depict flips.

Figure S5. Images of a cell with one Cy3 labeled SprB and three GldL-YFP foci. The track for the motion of SprB from movie S4 is plotted in Fig. 2A.

Figure S6. A simulation in which 42 motors were localized at random on one cell, with a frequency distribution of distances between the motors and the track. Inset shows the positions of the motors (green) and the track (red).

Figure S7. (A) Speed of a smooth gliding cell measured by tracking the center of mass of a gliding cell when plotted as a function of time does not change (Movie S6). **(B)** The speed of cell that displays two flips when plotted as a function of time show two sharp peaks (Movie S7).

Movie S1. A GldL-YFP strain displays wild-type levels of rotation. The cells attach to glass and beads coated with anti-SprB antibody attach to the cell.

Movie S2. A tethered cell with GldL foci.

Movie S3. CCCP stops cell rotation.

Movie S4. A Cy3-tagged SprB moving along the length of a cell.

Movie S5. An animation of the model suggesting how a molecular rack and pinion could drive gliding. The pinion is blue, the tread green, and the adhesin SprB is magenta.

Movie S6. A cell gliding smoothly over a glass surface.

Movie S7. A gliding cell displaying flips.

Supplementary Figures.

Figure S1.

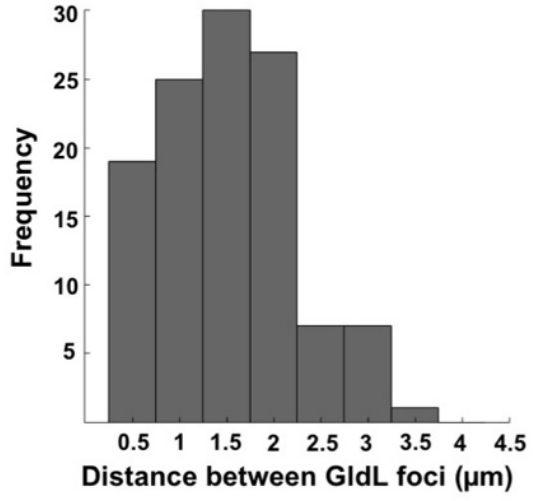

Figure S2.

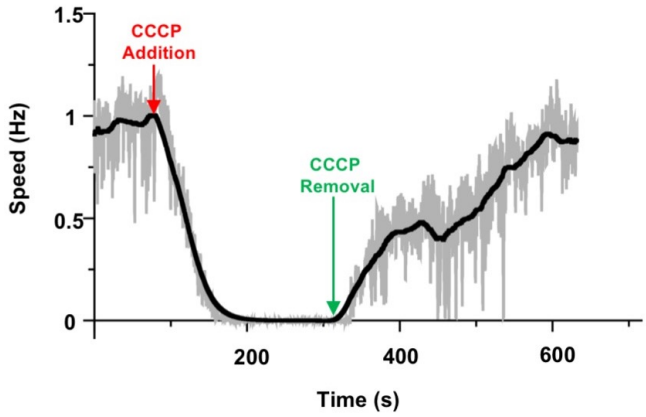

Figure S3.

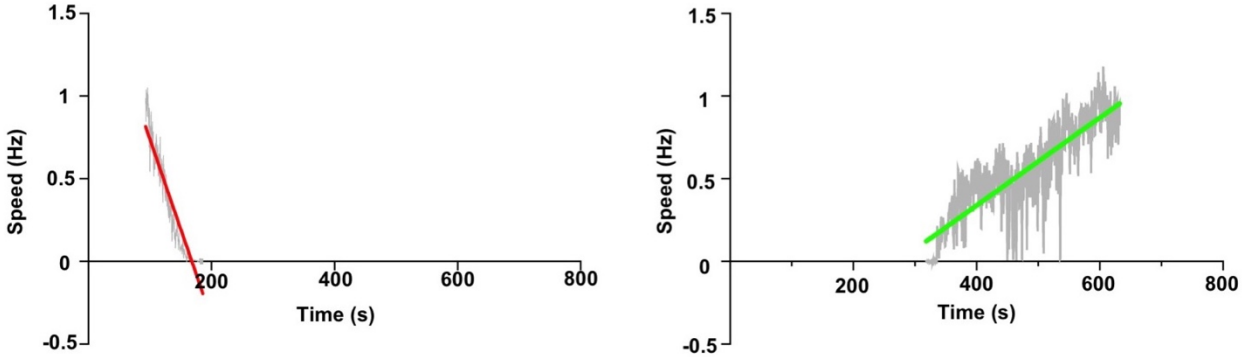

Figure S4.

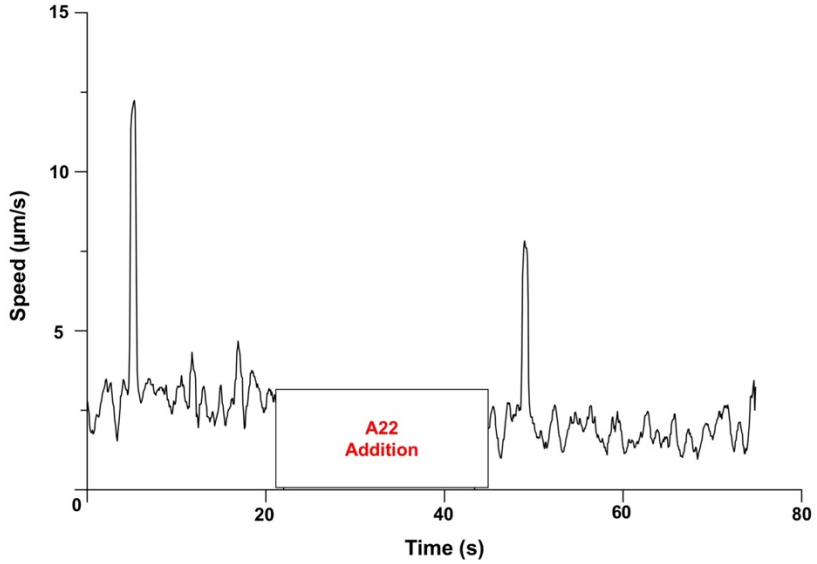

Figure S5.

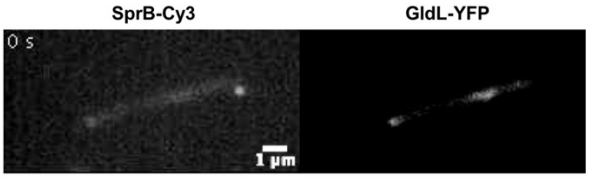

Figure S6.

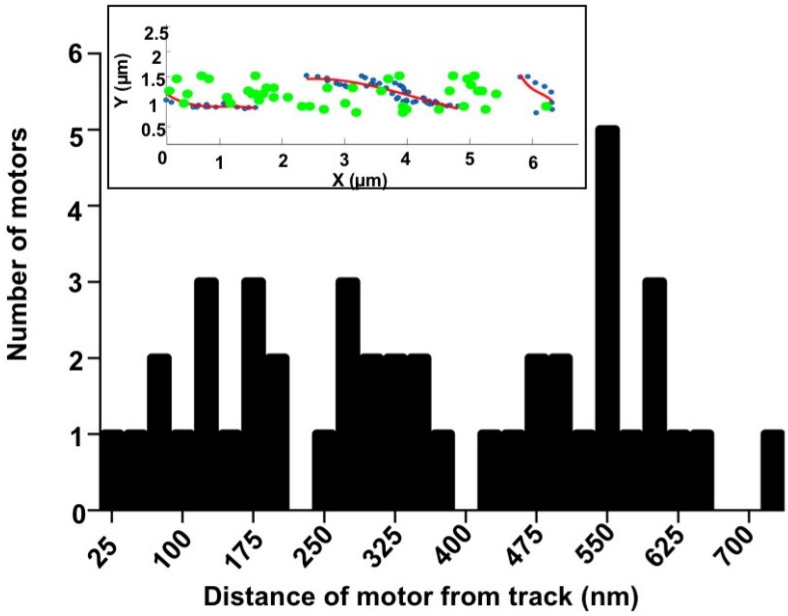

Figure S7.

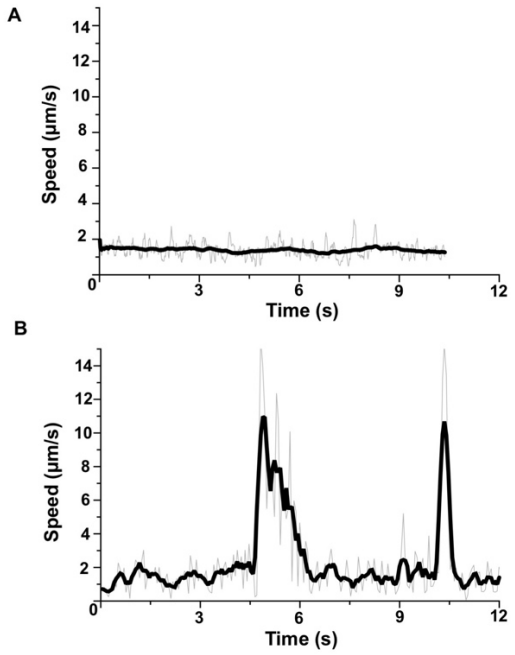

Primers used in the study

P63.
5' GCTAGGGTACCGGAACTCAAGTAACAGGAGGCG 3' forward primer upstream of gldL, KpnI site underlined.

P64.
5' GCTAGGGATCCTCCTTTGTTACTCATTGCAGAAAG 3' reverse primer in gldL, BamHI site underlined.

P65.
5'GCTAGGGATCC**GGAGGTGGA**ATGGTGAGCAAGGGCGAG 3'
Binds YFP start site in pHL55. BamHI site underlined, 3xG linker in bold.

P67.
5' GCTAGTCTAGA**TTA**CTTGTACAGCTCGTCCATGCCGAGAGTGATCCCGGCGGC 3'
Binds end region of yfp. Stop codon in bold. XbaI site underlined. *gldL-YFP* in the plasmid pCP23 was confirmed by sequencing.